Kinetics of the Low pH-Induced Conformational Changes and Fusogenic Activity of Influenza Hemagglutinin

Mathias Krumbiegel,* Andreas Herrmann,‡ and Robert Blumenthal*

*Section of Membrane Structure and Function, National Cancer Institute, National Institutes of Health, Bethesda, Maryland 20892 USA, and ‡Institute of Biophysics, Humboldt University, Berlin, Germany

ABSTRACT The decrease of the intrinsic tryptophan fluorescence intensity of purified influenza (X31 strain) hemagglutinin (HA) was used to monitor the low pH-induced conformational change of this protein. The kinetics of the fluorescence decrease depended strongly on the pH. At a pH optimal for fusion, the change in tryptophan fluorescence was fast and could be fitted to a monoexponential function. We measured a rate constant of 5.78 s^{-1} ($t_{1/2}$ = 120 ms) at pH 4.9 using rapid stopped-flow mixing. Under suboptimal conditions (higher pH), the rate constant was decreased by an order of magnitude. In addition, a slow component appeared and the fluorescence decrease followed a sum of two exponentials. The kinetics of conformational changes were compared with those of the fusion of influenza virus with red blood cell membranes as assessed by the R_{18}-dequenching assay. At optimal pH the HA conformational change was not rate-limiting for the fusion process. However, at sub-optimal pH, the slow transition to the fusogenic conformational of HA resulted in slower kinetics and decreased extent of fusion.

INTRODUCTION

Membrane fusion is an essential step in the infection of cells by influenza virus and allows the release of genetic information into the cell interior. The virus is endocytosed after binding to cell surface receptors. The low pH milieu inside the endosomes triggers a conformational change of a viral membrane protein, hemagglutinin (HA), that mediates fusion with the endosomal membrane (White, 1990). HA is an integral membrane protein that consists of two polypeptides (HA1 and HA2) linked by a disulfide bridge. HA is organized as a homotrimer within the viral membrane. The molecular structure of its ectodomain has been resolved by x-ray crystallography with a resolution of 3 Å (Wilson et al., 1981).

Although many details of the molecular rearrangement of HA at low pH have been described (see below), the fusogenic structure of HA and the molecular mechanism of subsequent membrane fusion remain to be elucidated. To examine the spatial and temporal structure of the fusion site, kinetic studies of lipid mixing as a result of fusion of enveloped viruses with target membranes have been performed. Mainly from those studies, it has been concluded that the HA-mediated fusion at low pH is a complex multistep process that encompasses a conformational change of the HA, the association of several HA-trimers to form a fusion site, and destabilization of the target membrane (Blumenthal et al., 1991). To characterize those intermediates and their dynamics, assays sensitive to the formation of such specific structures are required. The low pH state of HA was characterized by different methods: immunoprecipitation revealed the exposure of the predominantly hydrophobic N-terminus of HA2 ("fusion peptide") and some dissociation of the HA1 headgroups (White and Wilson, 1987), the protein becomes susceptible to proteolytic digestion (Skehel et al., 1982), morphological changes are observed by electron microscopy (Ruigrok et al., 1986;Puri et al., 1990), and liposome binding indicates an increased hydrophobicity (Doms et al., 1985). Such methods do not allow continuous monitoring of rapid kinetics, and extents of conformational transition may be underestimated because reneutralization is necessary for most of these assays.

A common way to investigate conformational changes of proteins is to monitor the intrinsic fluorescence of the tryptophan residues. The fluorescence properties are sensitive to the environment of tryptophan inside the protein and are influenced by factors as polarity, vicinity to quenching groups, and energy transfer acceptors (Lakowicz, 1983). A decrease of the tryptophan fluorescence of HA was observed when the pH was lowered (Sato et al., 1983; Wharton et al., 1988).

In the present study, we have extended such studies and have been able to monitor continuously the kinetics of the conformational change with a millisecond time resolution. Furthermore, we compared the pH dependence of the conformational change with those of the rates and extents of the fusion prossess as measured by the R_{18}-fluorescence assay (Hoekstra et al., 1984).

MATERIALS AND METHODS

Virus preparation

Influenza virus (strain X31) was grown for 48 h in 10-day-old embrionated hen eggs. The allantoic fluid of the eggs was collected, and cell debris was removed by a low speed spin. The virus was pelleted by spinning the allantoic fluid with 90,000 × *g* for 50 min. The pellet was homogenized with a teflon-coated homogenizer.

Received for publication 3 March 1994 and in final form 27 June 1994.

Address reprint requests to Dr. Robert Blumenthal, National Institutes of Health, 10 Center Dr., MSC1350 NCI, Bldg. 10, Rm. 4A-01, Bethesda, MD 20892-1350. Tel.: 301 496-8832; Fax: 301 402 3650; E-mail: blumen@helix.nih.gov.

Abbreviations used: R_{18}, octadecyl rhodamine B; HA, hemagglutinin; trp, tryptophan.

Dr. Krumbiegel's present address: Institute of Biophysics, Dept. of Biology, Humboldt University, 10115 Berlin, Germany.

0006-3495/94/12/2355/06 $2.00

Purification of HA

The viral membrane was solubilized in 1.5% octylgycoside (Pierce, Rockford, IL) for 1 h at 4°C. The insoluble material was removed by spinning at 100,000 × g for 60 min. The supernatant containing the hemagglutinin in detergent micelles was further purified by affinity chromatography on ricin A (Sigma Chemical Co., St. Louis, MO) according to Doms et al. (1985). The detergent and galactose were removed by dialysis against PBS for about 14 h with one buffer change. The purity of the hemagglutinin was checked by SDS-PAGE with 12% gels under reducing conditions and was judged to be at least 95% pure.

Tryptophan fluorescence measurements

Fluorescence measurements were performed on a SLM spectrofluorimeter (SLM-Aminco, Urbana, IL) at 37°C. Tryptophan was excited at 295 nm. To monitor fast kinetics, stopped-flow measurements were performed on a SFM-3 stopped-flow device (Bio-Logic, Claix, France). 25 μl of HA in PBS (~1 mg/ml) was mixed with 250 μl of PBS buffer with appropriate pH (adjusted with citric acid) to give the desired pH after mixing. Using a 31 μl quartz cuvette and a flow rate of 5.5 ml/s, the dead time amounted to about 2 ms. The trp fluorescence was measured by exciting at 295 nm from a SLM fluorescence spectrometer and monitoring the emission through a cutoff filter with a photomultiplyer tube at a time resolution of 1 ms. The data have been processed with the Biokine V3.20 software (Bio-Logic).

Changes in the tryptophan fluorescence were fitted to exponential function:

$$I(t) = I_A \exp(-k_A t) + I_B t) + I_\infty \quad (1)$$

where I_A and I_B correspond to the fluorescence intensities at zero time, I_∞ at infinite time, and $I(t)$ at any given time. Nonlinear curve-fitting was done using the software packages Sigma Stat and TableCurve (Jandel Scientific, San Rafael, CA). This program utilizes the Levenburg-Marquardt procedure for finding the global minimum of the χ^2 squared sum of deviations. We performed F statistics on the data that include a Normality test, Homoscedacity test, and Power or Sensitivity test. All of these tests confirm the goodness of the fits by the chosen models, monoexponential and biexponential, respectively. In addition, we have performed the Durbin-Watson statistics, which is a measure of serial correlation between residuals. The results of this test for the fits indicate no correlation of the residuals confirming that the models describe the data adequately.

Labeling of influenza virus and binding to erythrocyte ghosts

2 μl of 1 mg/ml R_{18} (in ethanol) was added under vortexing to 1 ml of virus suspension containing 1 mg of protein. After incubation for 10 min at room temperature, unbound R_{18} was removed by elution from a Sephadex G25 PD10 column (Pharmacia, Piscataway, NJ). Fresh erythrocyte ghosts were prepared from 0.5 ml of 50% washed red blood cells by hypotonic lysis with 5 mM phosphate buffer, pH 8, then washed twice with PBS. The labeled virus was then incubated with ghosts for 20 min on ice. After two washes with cold PBS, the pellet was resuspended in 0.5 ml of PBS.

Fusion assay

The R_{18} fluorescence was measured using a SLM 8000 spectrofluorimeter (SLM-Aminco, Urbana, IL) at 560 and 590 nm excitation and emission wavelength, respectively. 2 ml of PBS buffer at preadjusted pH and 37°C was placed in the fluorescence cuvette and stirred. Microliter amounts of virus/ghost complexes were rapidly added, and the fluorescence ($F(t)$) was monitored with a time resolution of 1 s. The maximal dequenching was obtained by adding 0.1% Triton X-100 (F_T). The dequenching was calculated from the following equation according to Blumenthal et al. (1987): percent dequenching = $(F(t) - F_0)/(F_T - F_0) \times 100$. F_0 is the initial fluorescence.

RESULTS

pH dependence of the intrinsic tryptophan fluorescence

The intrinsic tryptophan fluorescence of hemagglutinin is markedly reduced when the pH is lowered. In Fig. 1 the tryptophan fluorescence at 340 nm measured 60 min after incubation at the given pH (and 37°C) is shown. Concomitantly, the maximum of the intensity of the tryptophan spectrum is shifted to shorter wavelengths. The pH dependence of both the fluorescence intensity and the wavelength of maximum intensity give a sigmoidal curve with a half-value at about pH 5.5. To assess whether the fluorescence decrease at low pH can be restored, samples were reneutralized after different times (Fig. 2). The tryptophan fluorescence partially recovered to its original value after reneutralization after brief exposure to low pH as shown in Fig. 2. The recovery was instantaneous, and the fluorescence did not change any further upon incubation for longer times at neutral pH. As can be seen, the extent of reversibility is diminished to less than 40% after 10 s incubation of HA at pH 4.9. This suggests that the decrease of tryptophan emission at low pH reflects rapid irreversible changes of the HA conformation. However, complete irreversibility was observed only after several min (Fig. 2).

In Fig. 3 the quenching of hemagglutinin by acrylamide is shown. The data could be fitted to linear Stern-Volmer plots: $F_0/F = 1 + K_{sv}C$ (F, F_0, trp fluorescence in the presence and absence of quencher; K_{sv}, Stern-Volmer quenching constant; C, acrylamide concentration). The quenching constants have been estimated from the slopes of the plots and gave values of 5.64 M^{-1} at pH 7.4 and 4.26 M^{-1} at pH 4.9.

Kinetics of tryptophan fluorescence decrease at low pH

To follow the kinetics of the conformational change, we measured the Δ(tryptophan fluorescence) after exposing HA to different pH values. Concentrated microliter amounts of HA were added directly into the fluorescence cuvette, which contained buffer at 37°C with preadjusted pH (Fig. 4 A). A

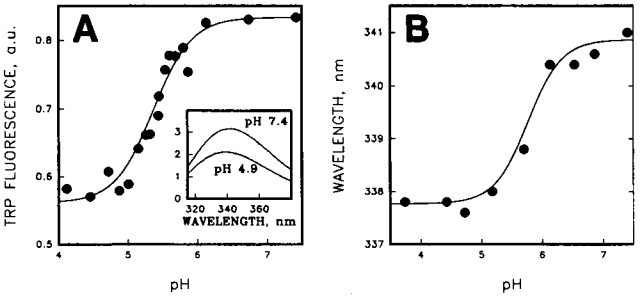

FIGURE 1 (A) Trp spectra of HA at neutral and low pH (*inset*) and pH dependence of the fluorescence intensity at 340 nm. (B) pH dependence of the wavelength of the intensity maximum. Measurements have been performed at 37°C with a protein concentration of 0.025 mg/ml. Tryptophan fluorescence was excited at 295 nm.

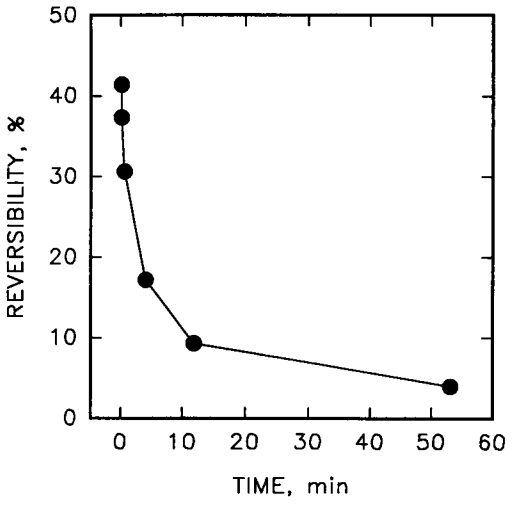

FIGURE 2 Reversibility of the tryptophan fluorescence intensity change of hemagglutinin at pH 4.9. The samples were reneutralized (by addition of microliter amounts of concentrated Tris) at different times after acidification as indicated. Conditions as described in Fig. 1.

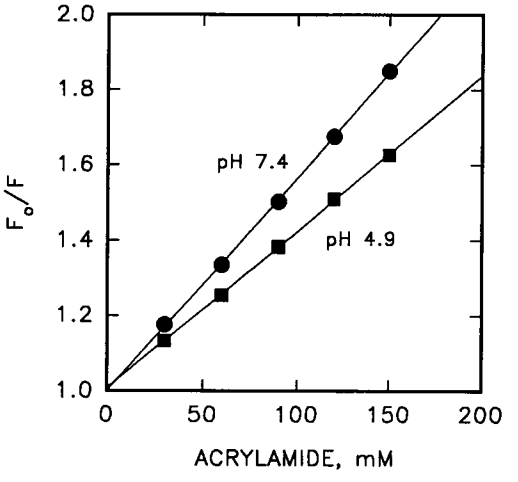

FIGURE 3 Stern-Volmer plots for quenching of hemagglutinin tryptophan fluorescence by acrylamide at different pH (experimental conditions as described in Fig. 1). F and F_0 represent the fluorescence intensity in the presence and absence of acrylamide, respectively. The quenching constants K_{sv} amount to 5.64 M^{-1} at neutral pH and 4.26 M^{-1} at pH 4.9.

distinct pH dependence with increasing rates at lower pH can be seen. The mixing time in the cuvette is about 2–4 s so that changes immediately after addition cannot be monitored. The kinetics at pH ≤ 5.1 was too rapid to observe the time dependence at all by this method. Thus, to catch the initial phase of the fluorescence decrease, stopped-flow measurements have been applied in this pH range (Fig. 4, *B* and *C*). At pH 4.9, 37°C, a fast decrease with a a rate constant of 5.78 s^{-1} (half-time of 120 ms) was observed, whereas at pH 5.1 the rate constant was 0.12 s^{-1} (see below). However, the fluorescence after a long time goes only down to 80% of the original fluorescence, whereas in the cuvette experiment (low time resolution, Fig. 4 *A*) a decrease to about 70% was

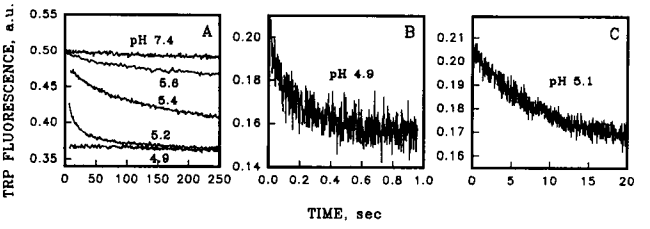

FIGURE 4 Kinetics of trp fluorescence of HA after exposing to low pH at 37°C. (*A*) Microliter amounts of HA suspension were added to milliliter volumes of stirred buffer solutions with different pH values as indicated (conditions as in Fig. 1). (*B*, *C*) Stopped-flow measurements of the trp fluorescence upon mixing with low pH buffer (details are described in Materials and Methods).

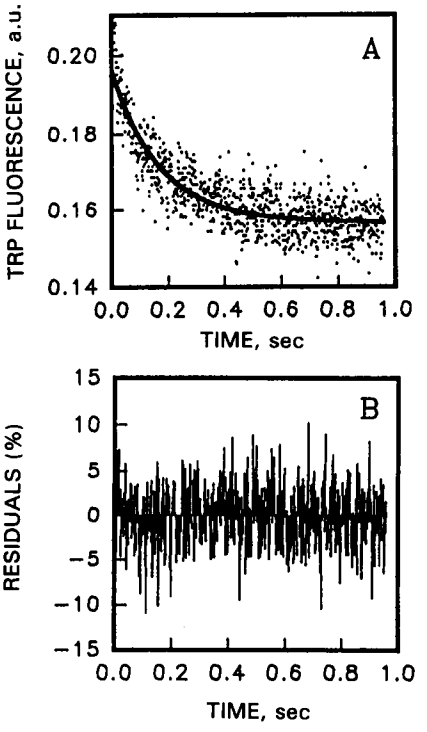

FIGURE 5 Fitting of the Δ(tryptophan fluorescence) of HA at pH 4.9, 37°C, by a monoexponential function (*A*) (see also Table 2). Residuals of curve-fitting are shown as percentage of measured values (*B*). The F statistic yielded values of 1670 and 869 for a monoexponential and biexponential fit, respectively. The higher number represents the best fit; normality and homoscedacity P values for the best fit were 0.146 and 0.892, respectively, and the Durbin-Watson statistics yielded a value of 1.2. The power of the test, representing the probability that the model correctly describes the relationship of the variables, was 0.999.

found. This suggests that a part of fluorescence decrease is still hidden in the dead time of the stopped-flow setup (~2 ms at the conditions used).

The curves were fitted to exponential functions, and the quality of the fits was deduced from values of F-statistics and from the magnitude as well as the absence of a systematic trend of the residuals. At pH optimal for fusion (pH 4.9–5.1; see Fig. 7), the decrease of the tryptophan fluorescence could be reasonably described by a monoexponential function

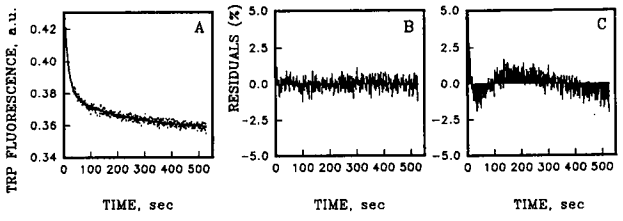

FIGURE 6 Fitting of the Δ(tryptophan fluorescence) of HA at pH 5.2, 37°C, by two exponential functions (see Material and Methods; Table 2) (*A*). Residuals of curve-fitting are given (*B*). For comparison, residuals of curve fitting by a monoexponential function are presented (*C*) showing a systematic trend. The F statistic yielded values of 2350 and 5258 for a monoexponential and biexponential fit, respectively. The higher number represents the best fit; normality and homoscedacity *P* values for the best fit were 0.046 and 0.623, respectively, and the Durbin-Watson statistics yielded a value of 1.7. The power of the test, representing the probability that the model correctly describes the relationship of the variables, was 0.999.

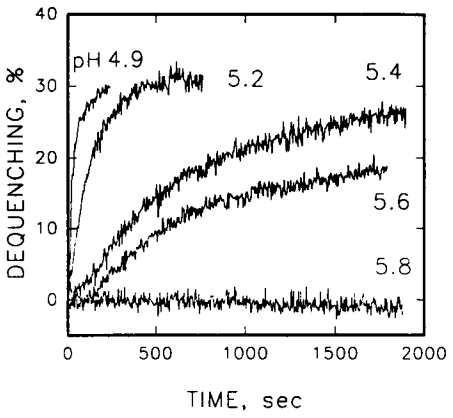

FIGURE 7 Fusion of influenza virus with erythrocyte ghosts at 37°C and different pH as indicated. Microliter amounts of suspensions containing virus-ghost complexes were added to milliliter volumes of stirred buffer solutions with preadjusted pH values.

(Fig. 5, pH 4.9; Table 1). Fitting to a sum of two exponential function does not reduce the magnitude of the residuals that were on the order of ≤5% of the measured values (Fig. 5 *B*). However, at pH > 5.1 feasible fitting of the Δ(tryptophan fluorescence) was only achieved by two exponential functions representing a fast and a slow component (Fig. 6) where the fraction of the slow component reaches ~75% at pH 5.6 (Table 1). Residuals of the monoexponential fit showed a systematic trend (Fig. 6 *C*). Although the rate constant of the fast component was on the order of 0.017 s^{-1} even at pH 5.6, those of the slow component increased from about 0.0044 (pH 5.2) to 0.00075 s^{-1} (pH 5.6) (Table 1).

To relate the kinetics of the conformational change of HA assessed by tryptophan fluorescence to HA-mediated membrane fusion, we have monitored the fusion of influenza virus with erythrocyte ghosts for different pH at 37°C (Fig. 7). Fusion was monitored by dequenching of the fluorescent probe R_{18} incorporated in the viral membrane (Hoekstra et al., 1984). Previously, we showed using stopped flow mixing techniques that the delay in onset of fusion was pH-dependent (Clague et al., 1991). Fig. 7 shows that the fusion extent is also pH-dependent, albeit to a lesser degree.

DISCUSSION

The intrinsic tryptophan fluorescence is often used as a marker for monitoring structural properties and conformational changes of proteins. In this study, we have utilized the fluorescence of tryptophan residues to follow the kinetics of the conformational change of influenza hemagglutinin (X31 strain) at low pH. The HA monomer of influenza X31 contains 12 tryptophan residues. Six trp belong to the HA2 subunit: two are located at the N-terminus, three in the transmembrane spanning part of HA2, and one in the middle part. The remaining six trp reside in the distal globular head of HA1 according to the three-dimensional structure of (Wilson et al., 1981).

Hemagglutinin undergoes a conformational change under mildly acidic conditions that triggers fusion between the viral and target membranes (White, 1990). As shown for the PR8 (Sato et al., 1983) and X31 strains of influenza (Wharton et al., 1988) the fluorescence intensity of HA decreases upon pH lowering, which has been associated with the conformational change. We observed a clear sigmoidal pH dependence for the intensity decrease as well as a blue-shift of the emission spectrum of HA of X31 (Fig. 1). The continuous loss of reversibility (Fig. 2) is consistent with independent assays that show that the conformational alterations of X31-HA at low pH are irreversible.

A common explanation for a blue-shift of the fluorescence spectrum is that tryptophan residues are becoming more buried and experience a more hydrophobic environment (Lakowicz, 1983). Usually, a more apolar environment is

TABLE 1 Kinetics of the conformational changes of HA

	Fast component		Slow component	
pH	k_A s^{-1}	Fractional amplitude (%)	k_B s^{-1}	Fractional amplitude (%)
5.6	0.017	26	$7.5\ 10^{-4}$	74
5.4	0.020	34	$2.7\ 10^{-3}$	66
5.2	0.067	75	$4.4\ 10^{-3}$	25
5.1	0.12	(monoexp. fit)		
4.9	5.78	(monoexp. fit)		

The curves generated from stopped-flow mixing experiments shown in Figs. 4–6 were fitted to Eq. 1. At pH values optimal for fusion (pH 4.9, 5.1) the curves were described by a monoexponential function, whereas at suboptimal pH values two exponential functions were required. Fractional amplitudes were derived from the preexponential factors (I_A and I_B) whose sum was normalized to 100%. Curve-fitting was done using the software TableCurve (Jandel Scientific, San Rafael, CA).

accompanied by an increase of the emission intensity as shown for tryptophan-containing model compounds (Brand and Withold, 1967). However, there is no strict relationship between maximum wavelength and tryptophan exposure in proteins caused by other factors such as internal quenching processes (Kronman and Holmes, 1971). A reduced exposure of tryptophans as an exclusive cause for the blue-shift would be somewhat surprising because immunoprecipitation (White and Wilson, 1987), electron microscopy (Puri et al., 1990), CD and DSC data (Krumbiegel et al., 1994, unpublished data) reveal a more unfolded and mobile structure with increased surface accessibility at low pH. The irreversibility of the fluorescence decrease excludes a quenching simply by protonation of adjacent groups. An alternative explanation for the blue-shift of the fluorescence is selective quenching of tryptophans located at or close to the surface of the protein. The conformational change possibly leads to a closer vicinity and/or an increased rate of contacts of those tryptophan residues to quenching groups as carboxyl groups, aminogroups, S-S-bonds and others located mainly at the surface of proteins. Our data are in agreement with Wharton et al. (1988), who could describe tryptophan quenching of BHA as well as rosettes with a single Stern-Volmer quenching constant. Looking at the crystal structure of HA (Wilson et al., 1981) it appears that eight out of the nine trp residues of BHA are located at the surface and thus should be accessible to quencher. Only one trp residue (trp-92) is completely buried inside the protein. Wharton et al. (1988) have obtained emission spectra from different tryptic fragments of HA after digestion by trypsin. They find that trp-92 has a very high fluorescence intensity that is preserved at low pH, whereas other trp residues have lower intensity that is reduced at low pH. This would also explain the reduced Stern-Volmer constant for acrylamide quenching at low pH. It is known that acrylamide preferentially quenches exposed tryptophan residues. If those groups are already quenched in the low pH conformation of HA, the Stern-Volmer constant for acrylamide quenching should be smaller because the access to internal tryptophans is lower.

The novel feature of this study is the measurement of the kinetics of the low pH-induced conformational change of HA using stopped-flow mixing techniques. We show that the kinetics of the conformational change of HA at pH optimal for fusion (pH $\leq$ 5.1, 37°C) can be monitored by the tryptophan emission. This method allows a time resolution on the order of 1 ms. This resolution cannot be attained by other assays sensitive to the conformational change that has been reported in the literature, e.g., proteolytic digestion (Doms et al., 1985), accessibility to antibodies White and Wilson, 1987), and liposome binding Stegmann et al., 1990). Those methods often require reneutralization and are sensitive only to the final state of a conformational change, e.g., the binding of antibodies to peptide sequences of HA becoming exposed at low pH, rather than to intermediate structures.

At pH 4.9 the conformational change was very fast with rate constant of 5.78 s^{-1} ($\tau_{1/2}$ = 120 ms), whereas at pH 5.1 the rate constant decreased by an order of magnitude. We have fitted the curves to exponential functions. Although at optimal pH the Δ(tryptophan fluorescence) could be fitted to a monoexponential function, kinetics of fluorescence decrease at suboptimal pH (>5.1) could only be reasonably approximated by a sum of two exponential functions, representing a fast and a slow component.

How do these conformational changes relate to kinetics of HA-mediated fusion? We have previously performed stopped flow kinetic measurements influenza viral fusion with erythrocyte ghosts at different pH values with 50 ms time resolution (Clague et al., 1991). The kinetics indicate that fusion does not follow a simple exponential behavior as would be expected from an instantaneous establishment of lipid continuity. The kinetics show a rather complex structure reminiscent of ion gating kinetics. At pH values close to threshold, a lag time of a few seconds was followed by a relatively slow rise. The lag time decreased and the rise time increased as the pH came closer to optimum. We interpret the lag time as reflecting the relative rates of rearrangements into the fusogenic state where membrane mixing takes place. The final extents of fusion are also pH-dependent as shown in Fig. 7. In analogy with ligand-induced activation of allosteric enzymes or of receptor-linked ion channels, we have modeled the process in terms a proton-driven shift of HA from a "T" (tense) state at neutral pH, to a series of "R" (relaxed) states (Blumenthal et al., 1989). The nature of a particular R state will not only determine the rate with which the system will be driven to a particular F state (fusion pore opening), but also the efficiency. Four representative conformers (R states) of HA are shown below as an example.

$$\begin{array}{ccccccc} T & \rightarrow & R_1 & \rightarrow & R_2 & \rightarrow & R_3 \rightarrow R_4 \\ & & \downarrow & & \downarrow & & \downarrow \quad \downarrow \\ & & F_1 & & F_2 & & F_3 \quad F_4 \end{array} \qquad (2)$$

Table 2 summarizes delay times leading to fusion (F states) taken from stopped flow data by [14] and rates of conformational changes for the four representative states. The kinetic data on the HA conformational change taken together with the stopped flow data of HA-induced fusion (Clague et al., 1991) allows us to determine the rate-limiting step at various pH values. The % conversion of the fast component to the active state equals $100\times(1 - e^{-k_A t})$. Substituting the delay time d for t yields % HA converted to the relevant R state at the onset of fusion = $100\times1 - e^{-k_A d}$). Table 2 shows that at pH 4.9, 99.7% is converted to its fusogenic confor-

TABLE 2 Relationship between kinetics of HA conformational changes and fusion

pH	State	Delay (s)*	% Converted‡
5.4	R1	4	7.7
5.2	R2	3	18.2
5.1	R3	2	21.3
4.9	R4	1	99.7

* From Clague et al. (1991).

‡ % converted = 100×(MATH), where k_A is the rate constant for the fast component (Table 1, column 2) and d is the delay time (Table 2, column 3).

mation (R4 state) before fusion starts, indicating that at optimal pH events leading to F (fusion pore formation) are rate-limiting. This is consistent with low temperature HA fusion data, which indicate that the conformational change occurs within 1 min (Stegmann et al., 1990; Pak et al., 1994), whereas the delay for the onset of fusion is about 10 min. At pH 5.1 (R3 state) only 21% is converted before fusion pore formation. At pH values close to threshold (5.2 and 5.4), only a relatively small proportion of HA is converted to the fusogenic state at the onset of fusion. It is interesting to note that the slower conversion to the fusogenic state also leads to inefficient assembly of the fusion pore and lower extent (see Fig. 7).

According to a model recently proposed by Carr and Kim (1993), the native state of HA is metastable ("spring-loaded") and the low pH induces a transition to a more stable final state. In this state, the fusion peptides are relocated 100 Å from their original position and face the target membrane immediately after exposure of HA to low pH. The model is based on an elegant study in which these investigators have identified a sequence in the HA2 subunit that has the propensity to form a coiled coil. The model is consistent with the crystallographic result by Wiley's group that demonstrates that this particular sequence forms an extended α helix (Bullough et al., 1994). We find that at optimal pH the "unzipping" of HA occurs rapidly, which is consistent with a rapid release of the springload. Moreover, the final state is arrived at rapidly, which implies that the system does not have to do an extensive conformational search to arrive at this state. However, at suboptimal pH values the "unzipping" of HA occurs hesitantly and stops at a different level of Δ(tryptophan fluorescence) than that at optimal pH. It would be of interest to reconcile this observation with the current paradigm that requires complete "unzipping" of HA to occur to form the coiled coil structure. The kinetic data therefore represent important factors that have to be taken into account in the evaluation of the mechanism by which HA mediates membrane fusion.

We thank Dr. Jay Knutson, Keith Kalmbach, and Denise Potter for support in performing the stopped-flow measurements.

REFERENCES

Blumenthal, R., A. Bali-Puri, A. Walter, D. Covell, and O. Eidelman. 1987. pH-dependent fusion of vesicular stomatitis virus with vero cells: measurement by dequenching of octadecylrhodamine fluorescence. *J. Biol. Chem.* 262:13614–13619.

Blumenthal, R., A. Puri, D. P. Sarkar, Y. Chen, O. Eidelman, and S. J. Morris. 1989. Membrane fusion mediated by viral spike glycoproteins. *In* Cell Biology of Virus Entry, Replication, and Pathogenesis. R. W. Compans, A. Helenius, and M. B. A. Oldstone, editors. Alan R. Liss, Inc., New York. 197–217.

Blumenthal, R., C. Schoch, A. Puri, and M. J. Claque. 1991. A dissection of steps leading to viral envelope protein-mediated membrane fusion. *Ann. N. Y. Acad. Sci.* 635:285–296.

Brand, L., and B. Withold. 1967. Fluorescence measurements in studies of protein conformation. *Methods Enzymol.* 11:776–856.

Bullough, P. A., F. M. Hughson, J. J. Skehel, and D. C. Wiley. 1994. Structure of influenza haemagglutinin at the pH of membrane fusion. *Nature* 371:37–43.

Carr, C. M., and P. S. Kim. 1993. A spring-loaded mechanism for the conformational change of influenza hemagglutinin. *Cell.* 73:823–832.

Clague, M. J., C. Schoch, and R. Blumenthal. 1991. Delay time for influenza hemagglutinin-induced membrane fusion depends on the haemagglutinin surface density. *J. Virol.* 65:2402–2407.

Doms, R. W., A. Helenius, and J. White. 1985. Membrane fusion activity of the influenza virus hemagglutinin: The low pH-induced conformational change. *J. Biol. Chem.* 260:2973–2981.

Hoekstra, D., T. de Boer, K. Klappe, and J. Wilschut. 1984. Fluorescence method for measuring the kinetics of fusion between biological membranes. *Biochemistry.* 23:5675–5681.

Kronman, M. J., and L. G. Holmes. 1971. The fluorescence of native, denatures and reduced-denatured proteins. *Photochem. Photobiol.* 14: 113–134.

Lakowicz, J. R. 1983. Principles of Fluorescence Spectroscopy. Plenum Press, New York.

Pak, C. C., M. Krumbiegel, and R. Blumenthal. 1994. Intermediates in Influenza PR/8 Hemagglutinin-induced Membrane Fusion. *J. Gen. Virol.* 75:395–399.

Puri, A., F. Booy, R. W. Doms, J. M. White, and R. Blumenthal. 1990. Conformational changes and fusion activity of influenza hemagglutinin of the H2 and H3 subtypes: effects of acid pretreatment. *J. Virol.* 64: 3824–3832.

Ruigrok, R. W., S. R. Martin, S. A. Wharton, J. J. Skehel, and P. M. Bayley. 1986. Conformational changes in the hemagglutinin of influenza virus which accompany heat-induced fusion of virus with liposomes. *Virology.* 155:484–497.

Sato, S. B., K. Kawasaki, and S. Ohnishi. 1983. Hemolytic activity of influenza virus hemagglutinin glycoprotein activated in mildly acidic environments. *Proc. Natl. Acad. Sci. USA.* 80:3153–3157.

Skehel, J. J., P. M. Bayley, E. B. Brown, S. R. Martin, M. D. Waterfield, J. M. White, I. A. Wilson, and D. C. Wiley. 1982. Changes in the conformation of influenza virus hemagglutinin at the pH optimum of virus-mediated membrane fusion. *Proc. Natl. Acad. Sci. USA.* 79:968–972.

Stegmann, T., J. M. White, and A. Helenius. 1990. Intermediates in influenza-induced membrane fusion. *EMBO J.* 9:4231–4241.

Wharton, S. A., R. W. Ruigrok, S. R. Martin, J. J. Skehel, P. M. Bayley, W. Weis, and D. C. Wiley. 1988. Conformational aspects of the acid-induced fusion mechanism of influenza virus hemagglutinin. Circular dichroism and fluorescence studies. *J. Biol. Chem.* 263:4474–4480.

White, J. M. 1990. Viral and cellular fusion proteins. *Annu. Rev. Physiol.* 52:675–697.

White, J. M., and I. A. Wilson. 1987. Anti-peptide antibodies detect steps in a protein conformational change: low-pH activation of the influenza virus hemagglutinin. *J. Cell Biol.* 56:365–394.

Wilson, I. A., J. J. Skehel, and D. C. Wiley. 1981. Structure of the hemagglutinin membrane glycoprotein of influenza virus at 3 Å resolution. *Nature.* 289:366–373.